Available online at www.sciencedirect.com

SciVerse ScienceDirect

Ceramics International 39 (2013) 4081–4087

CERAMICS
INTERNATIONAL

www.elsevier.com/locate/ceramint

Preparation and characterization of crednerite glass–ceramics in the $MnO \cdot CuO \cdot SiO_2$ system

Salwa A.M. Abdel-Hameed, Fatma H. Margha*

Glass Research Department, National Research Center, Dokki, Cairo 12311, Egypt

Received 24 September 2012; received in revised form 27 October 2012; accepted 29 October 2012
Available online 5 November 2012

Abstract

Nanoscale crednerite ($CuMnO_2$) was prepared in the system $MnO \cdot CuO \cdot SiO_2$, using glass–ceramics technique for the first time. Based on obtained data from differential thermal analysis (DTA), the prepared samples were heat-treated at 700 and 800 °C for 2 h. The presence of crystalline phases after and before heat treatment was investigated by X-ray diffraction analysis. Crystallization of crednerite ($CuMnO_2$), manganese silicate (Mn_2SiO_4) and traces of cuprite (Cu_2O) and cristobalite (SiO_2) phases were recognized. Transmission electron microscopy showed nanoscale crystals in the range 5–10 nm. The prepared glass–ceramics showed ferrimagnetic properties with wide range coercivity from 53 to 2217 Hci and magnetization saturation from 0.21708 to 1.2 emu/g. From IR reflection data; the reflection intensity of the light is high in the range of orange–red color and violet–blue colors and low in the range of green color.

Keywords: C: Magnetic properties; D: Glass ceramics; Crednerite

1. Introduction

$A^+B^{3+}O_2$ family, (A is commonly a monovalent metal and B any one of 3d transition metals [1,2]), derived from the delafossite structure, is characterized by many advanced properties that make it very interesting for engineering applications. For example, it is characterized by moderate band gap energy ($E_g = 1.4$ eV) that confers them an efficient use of the solar spectrum. $CuBO_2$, where B is 3d element is a p-type semiconductor (SC) that could be used in practical applications to convert the light to chemical energy and was confirmed recently by its use as H_2-electrode under visible light [3,4]. Also, its electric properties were slightly improved by the doping process [5]. However, it is well established that the electrical and magnetic properties of $CuBO_2$ strongly depend on the preparative conditions and particularly on the structure type of the precursor [6].

$CuMnO_2$, called crednerite, has a monoclinic structure with C2/m space group; it is distorted from the hexagonal delafossite structure due to the Jahn–Teller effect of Mn^{3+} ions that have crystal-field splitting in eg orbitals due to d4 electronic configuration. Bulk $CuMnO_2$ shows three dimensional antiferromagnetic spin ordering at low temperatures in spite of the anisotropic crystal structure [7].

In this paper we focus on the preparation of crednerite ($CuMnO_2$) by the glass–ceramics technique for the first time. The crystallization of crednerite ($CuMnO_2$) was studied and its effect on the magnetic and optical properties was also investigated.

2. Experimental methods

2.1. Preparation of the glass

Chemical compositions of samples under investigation are given in Table 1. The compositions are designed to study the effect of CuO and MnO content on the sequence of crystallization in the system $MnO \cdot CuO \cdot SiO_2$. Samples are denoted by M0, M1 and M2, where M0 contains equal amount of both MnO and CuO (~35 mol%) and it was regarded as the base composition while M1 contains more CuO (~50 mol%) and M2 contains more MnO (~50 mol%). Our target was to obtain a glass–ceramic not a ceramic material, so a melting step was necessary to achieve the nucleation process in the

---

*Corresponding author. Tel.: +20 2 33371362; fax: +20 2 33387803.
E-mail address: fatmamargha@yahoo.com (F.H. Margha).

0272-8842/$ - see front matter © 2012 Elsevier Ltd and Techna Group S.r.l. All rights reserved.
http://dx.doi.org/10.1016/j.ceramint.2012.10.262

Table 1
Chemical composition of glass samples in mole %.

Sample	Composition (mol%)		
	MnO	CuO	SiO_2
M0	35	35	30
M1	20	50	30
M2	50	20	30

liquid-derived amorphous phase. After well mixing of 100 g of each composition for 15 min in ball miller, the batches were melted in a Pt crucible in an electrically heated Globar furnace at 1200 °C for 3 h with occasional swirling every 30 min to ensure homogenization. The melts were poured on to a stainless steel plate at room temperature and pressed into a plate 1–2 mm thick by another cold steel plate.

2.2. Crystallization of the glasses

Thermal behavior of the finely powdered glass samples was examined using SETRAM Instrumentation Reulation, Labsys™ TG-DSC16 under inert gas. The powdered glass was heated in Pt-holder with another Pt-holder containing Al_2O_3 as a reference material. The results obtained were used as a guide for determining the required heat-treatment temperatures needed to induce crystallization in the samples. Heat treatment schedules were carried out under reducing atmosphere by covering the samples by active carbon during heating to study the effect of reducing atmosphere on the sequence of crystallization.

2.3. Characterization

Samples before and after heat treatment were subjected to powder X-ray diffraction (XRD) using Ni-filled Cu-K_α radiation for the determination of the precipitated crystalline phases. XRD was performed using Bruker D8 Advanced Instrument (Germany D8 ADVANCE Cu target 1.54 Å, 40 kv, 40 mA). The reference data for the interpretation of the X-ray diffraction patterns was obtained from ASTM X-ray diffraction card files.

The heat-treated samples were crushed and sonically suspended in ethanol, few drops of the suspended solution were placed on an amorphous carbon film held by a copper microgrid mesh and then observed using JEM 2010 transmission electron microscope to study the microstructure and crystallite size.

The magnetic properties of the as prepared and heat treated samples were measured at room temperature using a vibrating sample magnetometer (VSM; 9600-1 LDJ, USA) in a maximum applied field of 20 kOe. From the obtained hysteresis loops, the saturation magnetization (M_s), remanance magnetization (M_r) and coercivity (H_c) were determined.

Fourier transform infrared (FTIR) was carried out using FT-IR spectrometer (type NEXUS FT-IR-AES 0100394-manufactured 2001, USA) with diffusive reflection attachment. The samples were measured in the wavenumber range of 400–2500 cm^{-1}.

3. Results

DTA results are obtained in Fig.1. DTA trace of the base composition M0 showed a deep endothermic effect at 338 °C followed by sharp and intense exothermic one at 803 °C. For sample containing more Cu ions (M1) the endothermic effect was shifted to higher temperature (~500 °C), while the exothermic effect was shifted to lower one (~610 °C) and became more intense. In M2 sample rich in Mn ions, DTA results showed endothermic effect at 500 °C as in case of M1 sample followed by two exothermic effects at both 618 °C and 685 °C.

Figs. 2–4 show the XRD patterns of samples, M0, M1 and M2, as quenched samples and after heat treatment at 700 and 800 °C for 2 h under air or reducing atmosphere.

Transmission electron microscopy (TEM) was performed in order to investigate the possibility of microtwinning and the homogeneity of the materials. TEM can determine exactly the size of each individual crystal. Also, particle size measurements can be viewed from TEM measurements in a sense of approximation Figs. 5–8.

From XRD study of the crystallized phases, it can be seen for crednerite as the only phase has ferrimagnetic magnetic properties while CuO, Cu_2O, SiO_2 and Mn-containing phases are regarded as anti-ferromagnetic materials. The hysteresis loops are measured under the magnetizing

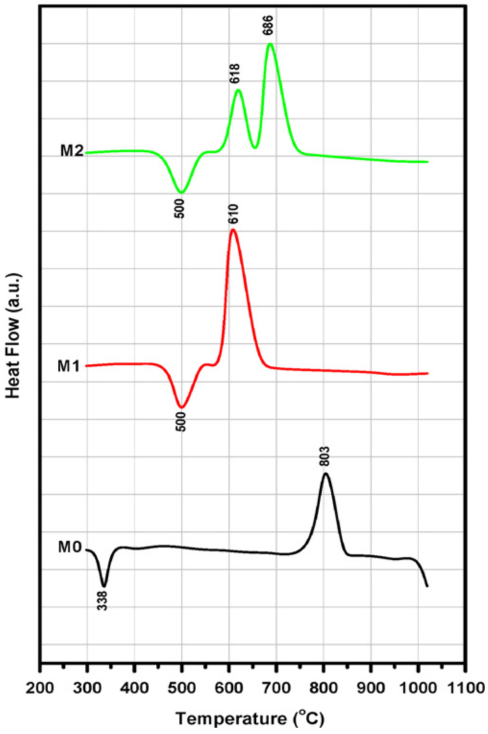

Fig. 1. DTA traces of M0, M1 and M2 samples without heat treatment.

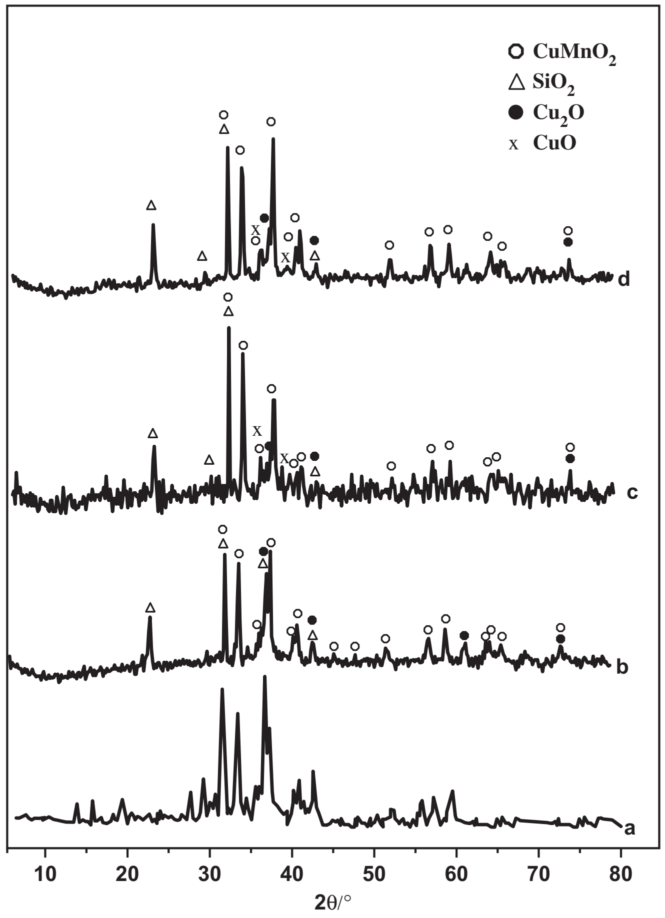

Fig. 2. XRD patterns of M0 sample at different heat-treatment conditions, (a) as quenched sample, (b) at 700 °C/2 h, (c) at 800 °C/2 h and (d) at 800 °C/ 2 h under reducing atmosphere.

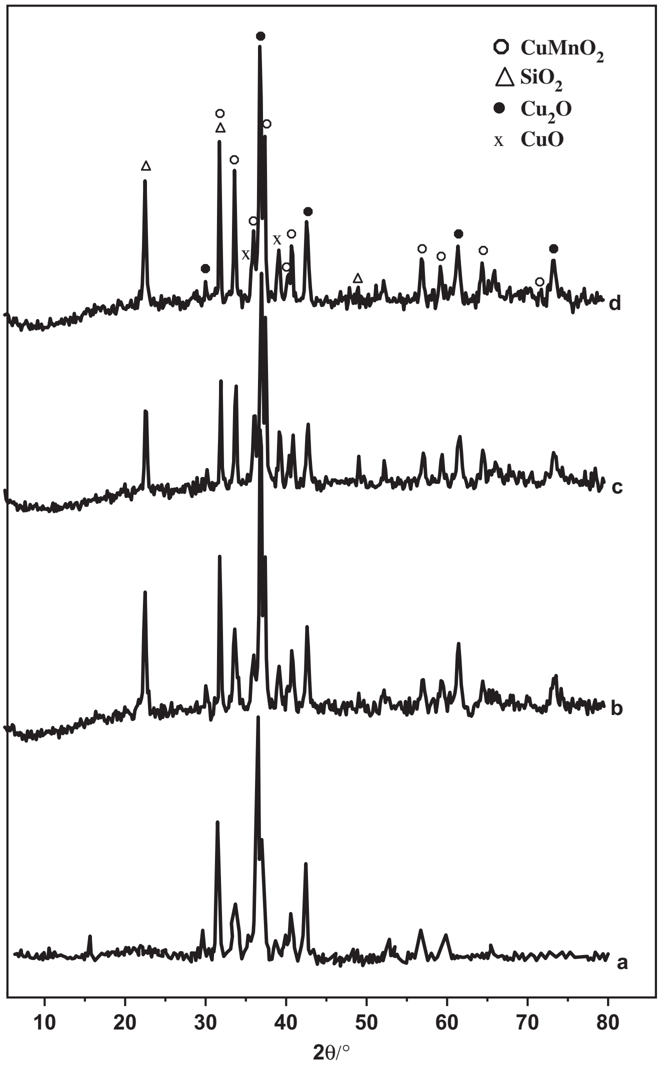

Fig. 3. XRD patterns of M1 sample at different heat-treatment conditions, (a) as quenched sample, (b) at 700 °C/2 h, (c) at 800 °C/2 h and (d) at 800 °C/2 h under reducing atmosphere.

field from $-20{,}000$ to 20,000 G at room temperature as shown in Figs. 9–11 and Table 2.

Table 3 shows the standardized intensity for the reflection spectra of crednerite in air for M0 sample heat treated at 700 °C for 2 h. It is noticed that the reflection intensity of the light increased in the range of orange–red color and violet–blue colors and decreased in the range of green color.

4. Discussion

4.1. *Differential thermal analysis*

The endotherm marks the glass transition (T_g) and softening temperatures (T_s) which are believed to be caused by an increase in heat capacity due to transformation of glass structure [8]. The exotherm reaction of crystallization effects, which is accompanied by releasing heat due to its lower free energy, reaches its maximum rate near the summit of the exothermal peak. The higher the intensity and sharpness of the exothermic peak is, the higher the propensity, velocity and bulk (internal) crystallization [9,10].It was found that, presence of more Cu ions in M1 enhances greatly the crystallization process. This is mirrored by the sharper, higher intensity and lower temperature of the exothermic peak of M1 sample when compared with M0. This result may be due to the lower ionic volume and the higher electronegativity of Cu than Mn. These two properties facilitate its mobility leading to easier crystallization process.

Presence of one exothermic effect may be related to crystallization of one or more phases in the same temperature range, while presence of two exothermic effects reflect crystallization of different phases in different temperature ranges. Accordingly, and as will be shown later in XRD analysis, the first exothermic effect appeared in M2 sample might be related to crystallization of both $CuMnO_2$ and Cu_2O; as in case of M0 and M1; while the second exothermic effect was related to crystallization of Mn-containing phases. Thus it can be concluded that both $CuMnO_2$ and Cu_2O have the same crystallization temperature range which is lower than the temperature needed for crystallization of Mn-containing phases.

4.2. X-ray diffraction analysis

In sample containing equal amounts of both MnO and CuO (M0); CuMnO$_2$, CuO$_2$ and SiO$_2$ phases were crystallized before and after heat treatment. CuMnO$_2$ was the predominant phase and its diffraction peaks were in good agreement with JCPDS card no. 75-1010, suggesting that the prepared CuMnO$_2$ is mainly crystallized in monoclinic structure. Increasing heat treatment temperature enhanced the development of crednerite phase. On contrary, Cu$_2$O phase decreased with the increase in the temperature of heat treatment (Fig. 2). Traces of CuO appeared in M0 sample heat treated at 800 °C for 2 h due to partial oxidation of cuprite (Cu$_2$O). Applying reducing atmosphere at the same temperature led to disappearance of CuO phase which is due to reduction of CuO to cuprite.

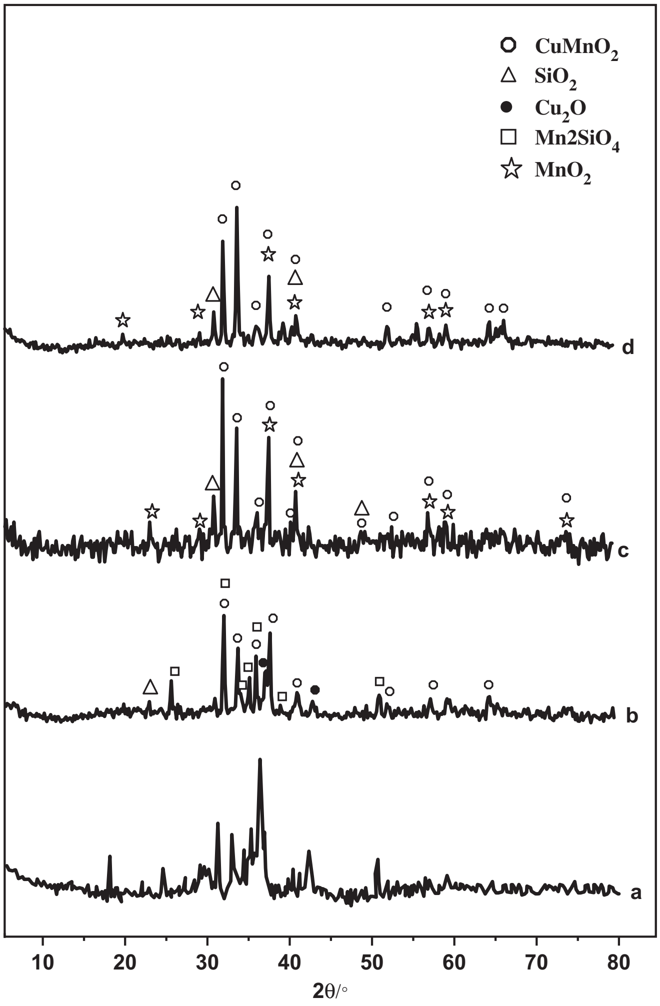

Fig. 4. XRD patterns of M2 sample at different heat-treatment conditions, (a) as quenched sample, (b) at 700 °C/2 h, (c) at 800 °C/2 h and (d) at 800 °C/2 h under reducing atmosphere.

In M1 sample, which contains more CuO than MnO, cuprite was crystallized as major phase followed by crystallization of CuMnO$_2$ (Fig. 3).Heat treatment of this sample at 700 °C, 800 °C for 2 h revealed appearance of SiO$_2$ and CuO as minor phases beside the above mentioned phases. The amount of CuO was decreased by applying reducing atmosphere as discussed before in case of M1. It is clear that cuprite (Cu$_2$O) is the main crystallized phase in M1 sample before and after heat treatment due to the high amount of CuO present in this composition.

XRD patterns of M2 sample (Fig. 4), which contains more MnO than CuO, revealed crystallization of cuprite and crednerite phases in the quenched sample. Heat treatment of this sample at 700 °C for 2 h led to the crystallization of CuMnO$_2$ as the major crystallized phase along with cuprite and SiO$_2$ as minor phases. Significant amount of Mn$_2$SiO$_2$ phase was also crystallized in this sample. Increasing the heat treatment to 800 °C for 2 h caused separation of traces of MnO$_2$ and SiO$_2$ phases (as a result of dissociation of Mn$_2$SiO$_2$) beside the major crystalline phase, CuMnO$_2$. Applying reducing atmosphere at 800 °C enhanced the crystallization process which was reflected by the increased intensity of XRD peaks related to the same crystallized phases in air at the same temperature.

4.3. Microstructure study using TEM

TEM of M0 heat treated at 800 °C for 2 h under reducing atmosphere (Fig. 5a) illustrated that the powder consists of

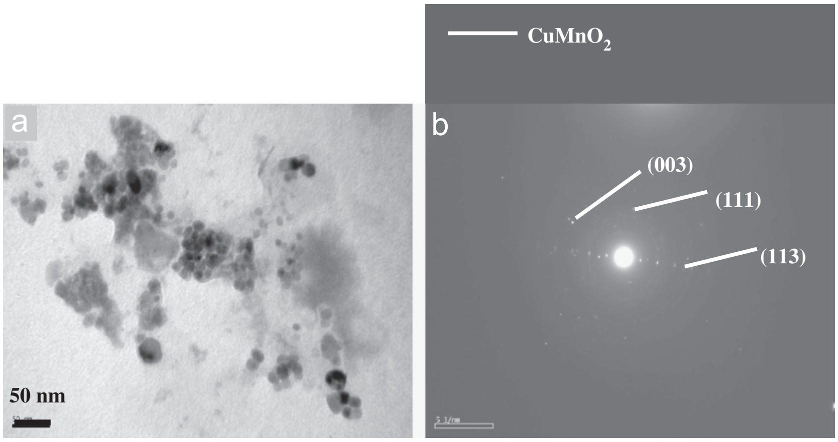

Fig. 5. TEM and diffraction rings of sample M0 heat treated at 800 °C/2 h under reducing atmosphere.

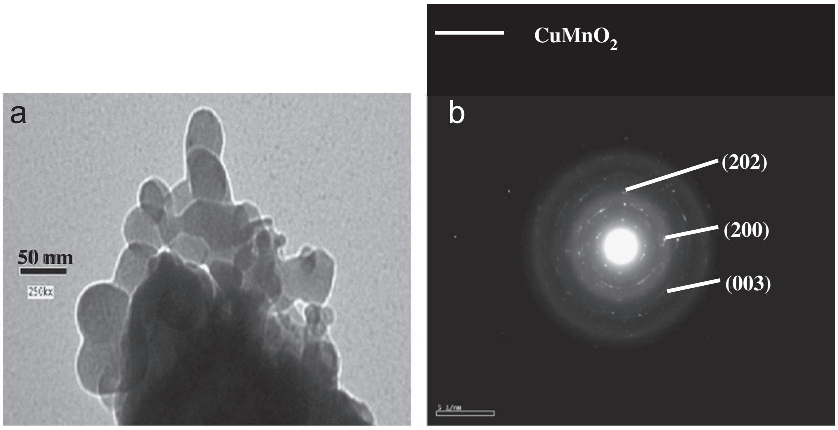

Fig. 6. TEM and diffraction rings of sample M1 heat treated at 800 °C/2 h under reducing atmosphere.

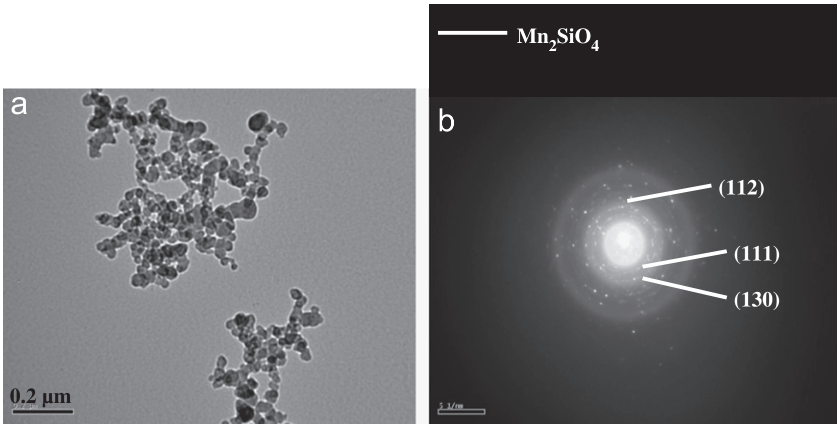

Fig. 7. TEM and diffraction rings of sample M2 heat treated at 700 °C/2 h.

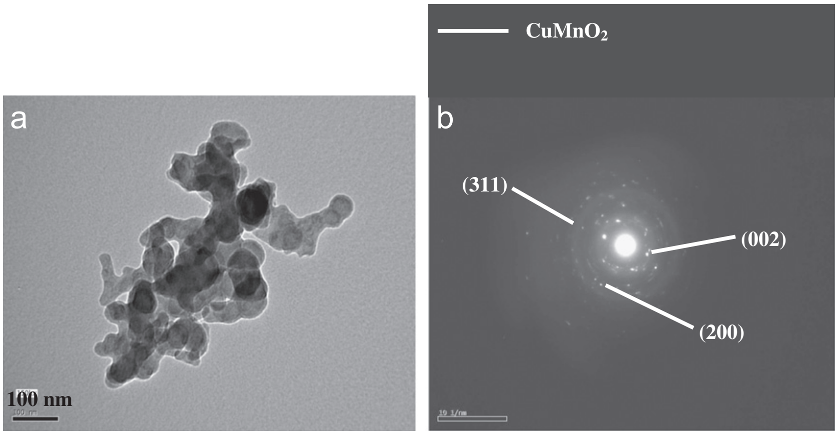

Fig. 8. TEM and diffraction rings of sample M2 heat treated at 800 °C/2 h under reducing atmosphere.

agglomerates of fine particles with a crystallite size less than 10 nm. However, the particle shapes are not well-defined suggesting that the powder is partially crystallized. The electron diffraction rings (Fig. 5b) were obtained at *hkl* 111 which is corresponding to the main diffraction peak of crednerite. TEM diffraction rings certified the pattern of crednerite structure as major crystallized phase with the two other crystallized phases (SiO$_2$ and cuprite). The major phase has been indexed as crednerite structure (*C2/m space group*) because of the presence of the three diffraction peaks (002, 200 and 111), which coincide with the diffraction peaks of monoclinic structure deduced from XRD data.

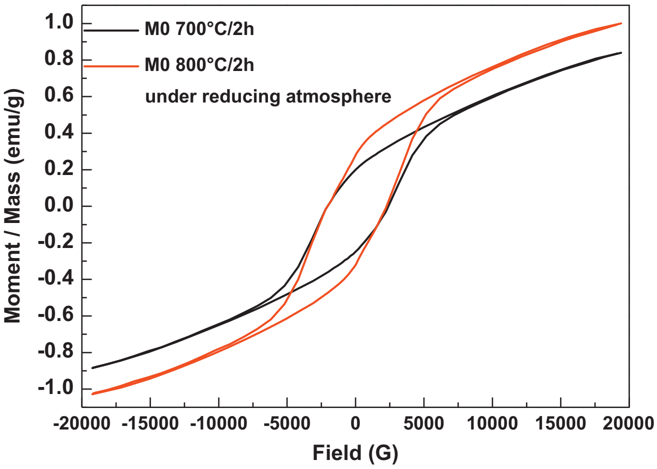

Fig. 9. Effect of heat treatments on the hysteresis loop of M0.

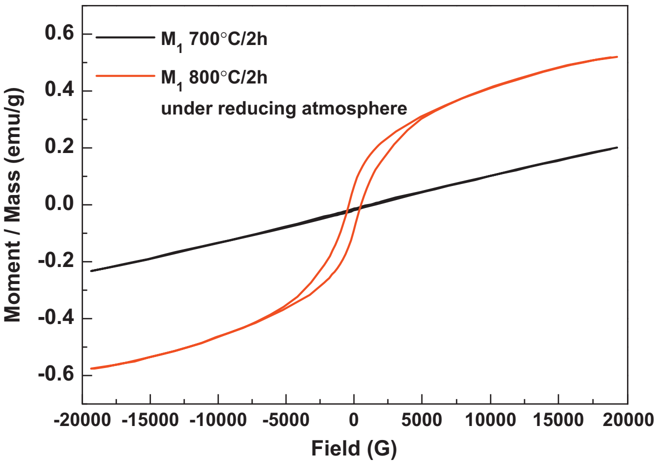

Fig. 10. Effect of heat treatments on the hysteresis loop of M1.

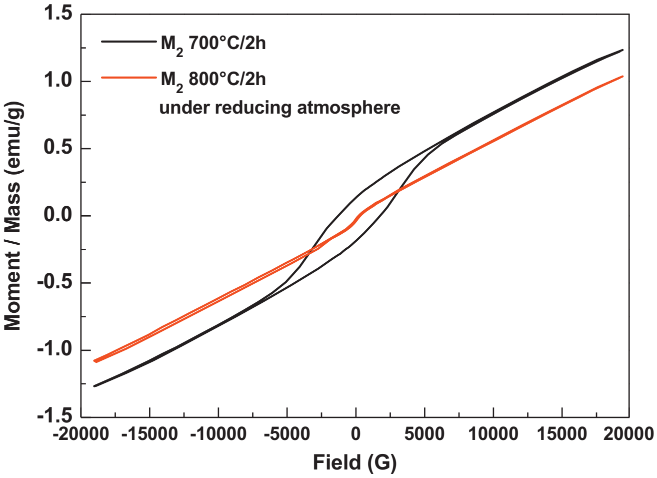

Fig. 11. Effect of heat treatments on the hysteresis loop of M2.

M1 sample heat treated at 800 °C for 2 h under reducing atmosphere exposed more development of the crystals confirmed by increasing the crystallite size to 46, 25 and 13.4 nm, which confirm presence of polycrystalline phases. More sharpness of diffraction lines were detected (Fig. 6).

Studying microstructure of M2 heat treated at 700 °C for 2 h revealed nanocrystallite size ~16.2 nm of well developed crystal of Mn_2SiO_2, crednerite, SiO_2, cuprite, and as confirmed by electron diffraction rings at (111, 130, 112 and 222) (Fig. 7). Increasing the temperature to 800 °C under reducing atmosphere brought about more development of the crystallized phases leading to increased crystallite size (Fig. 8).

4.4. *Magnetic behavior of the samples*

All the samples exhibited ferrimagnetism and the saturation magnetization increased with raising Mn concentration and consequently increasing in $CuMnO_2$ phase (Table 2).

The magnetization values of M0 and M2 samples were the highest due to the precipitation of $CuMnO_2$ phase. Meanwhile, M1 sample showed less magnetization value which was owed to the formation of Cu_2O.

The coercivity of these materials recorded high values ranging from 53 to 2217 Hci. In materials science, the coercivity of a ferromagnetic material is the intensity of the applied magnetic field required to reduce the magnetization of that material to zero after the magnetization of the sample has been driven to saturation. Coercivity measures the resistance of a ferrimagnetic material to become demagnetized.

The wide range of coercivity gives a wide range of applications. Materials with high coercivity which called hard ferrimagnetic materials are used to make permanent magnets. Permanent magnets find application in electric motors, magnetic recording media (e.g. hard drives, floppy disks, or magnetic tape) and magnetic separation. While a material with low coercivity which is said to be a soft magnet may be used in microwave devices, magnetic shielding, transformers, or recording heads.

The portion of the loop which lies in the second quadrant is known as the demagnetization curve. This is the portion of interest in a discussion of permanent magnets. In general, it is desirable that permanent magnets have a large remanence to retain a great of the magnetization, and a large coercive force in order that the magnet will not easily be demagnetized. Consequently, the retentivity which detects the amount of magnetic materials which can be magnetized, even in the absence of external magnetic field reaches higher values for M0 and minimum value for M1.

5. Conclusions

Crednerite with crystallite size 5–10 nm were prepared in the system MnO–CuO–SiO_2 via glass–ceramic technique for the first time. Prepared material is characterized by more homogeneous dispersed nanomagnetic particles immersed in amorphous phase than other conventional methods. The crystallization of credeinte, CuO_2 and SiO_2 phases were confirmed and increasing heat-treatment temperature revealed

Table 2
Magnetic results of samples under investigation.

Name of sample	Magnetization (emu/g)	Coercivity (G)	Retentivity (emu/g)
M0 700 °C/2 h	0.86236	2216.9	0.22468
M0 800 °C/2 h under reducing agent	1.0145	2038.3	0.28789
M1 700 °C/2 h	0.21708	179.72	2.8668×10^{-3}
M1 800 °C/2 h under reducing agent	0.54793	561.43	94.612×10^{-3}
M2 700 °C/2 h	1.2510	1531.4	0.16144
M2 800 °C/2 h under reducing agent	1.0627	53.575	7.1101×10^{-3}

Table 3
Standardized intensity (100%) reflection spectra of crednerite in air for sample M0 (700 °C/2 h).

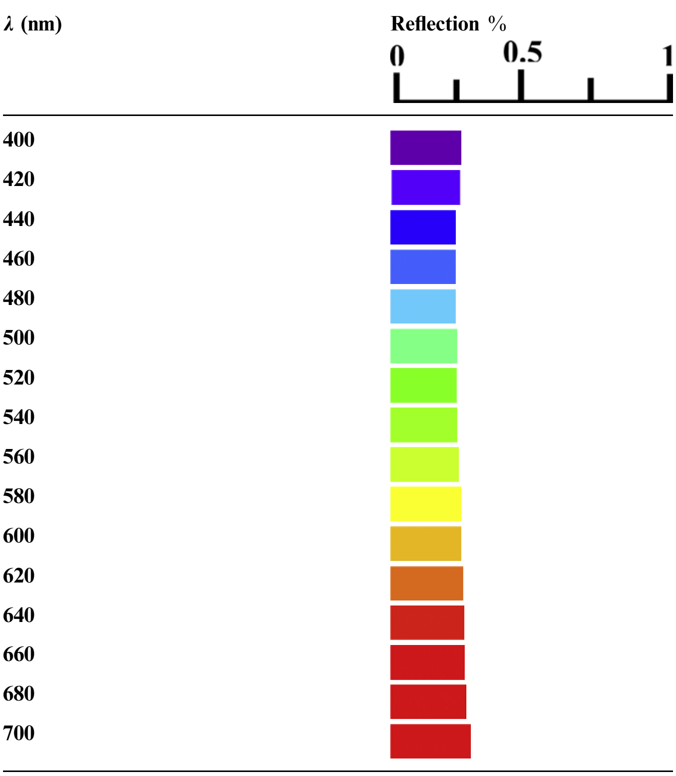

more development of credeinte phase. Applying reducing atmosphere at 800 °C increased the crystallization process which is reflected by increasing XRD intensity of the same crystallized phases in air at the same temperature. Crystal size of M0 sample was 9–10 nm, while for sample M1, crystal size was 46, 25 and 13.4 nm indicating the crystallization of three phases. For M2 sample, crystallite size was ~16.2 nm. From the obtained hysteresis loops, the saturation magnetization (M_s), remanance magnetization (M_r) and coercivity (H_c) were determined. All samples exhibited magnetic behavior characteristic for soft magnetic particles, with high coercivity from 53 to 2217 HCi, which gives a wide range of applications.

Acknowledgments

This work was supported financially by the Science and Technology Development Fund (STDF), Egypt, Grant no. 1044.

References

[1] Y. Bessekhouad, Y. Gabes, A. Bouguelia, M. Trari, The physical and photo electrochemical characterization of the crednerite $CuMnO_2$, Journal of Materials Science 42 (2007) 6469–6476.

[2] J. Li, A.W. Sleight, C.Y. Jones, B.H. Toby, Trends in negative thermal expansion behavior for AMO_2 (A=Cu or Ag; M=Al, Sc, In, or La) compounds with the delafossite structure, Journal of Solid State Chemistry 178 (2005) 285–294.

[3] M. Younsi, A. Aider, A. Bouguelia, M. Trari, Visible light-induced hydrogen over $CuFeO_2$ via $S_2O_3^{2-}$ oxidation, Solar Energy 78 (2005) 574–580.

[4] Y. Bessekhouad, M. Trari, J.P. Doumerc, $CuMnO_2$ a novel hydrogen photoevolution catalyst, International Journal of Hydrogen Energy 28 (2003) 43–48.

[5] R. Gall Bruce, N. Ashmore, M.A. Marquardt, T. Xiaoli, D.P. Cann, Synthesis microstructure, and electrical properties of the delafossite compound $CuGaO_2$, Journal of Alloys and Compounds 391 (2005) 262–266.

[6] J.Y. Shin, J.P. Doumerc, P. Dordor, C. Delmas, M. Pouchard, P. Hagenmuller, Influence of the preparation method and doping on the magnetic and electrical properties of $AgNiO_2$, Journal of Solid State Chemistry 107 (1993) 303–313.

[7] H. Hiraga, T. Fukumura, A. Ohtomo, T. Makino, A. Ohkubo, H. Kimura, M. Kawasaki, Optical and magnetic properties of $CuMnO_2$ epitaxial thin films with a delafossite-derivative structure, Applied Physics Letters (2009) id. 032109 (3 pages).

[8] K. Watanable, E.A. Giess, Crystallization kinetics of high-cordierite glass., Journal of Non-crystal Solids 169 (1993) 306–310.

[9] A.W.A. El-Shennawi, A. Mandour, M.M. Morsi, S.A.M. Abdel-Hameed, Monopyroxenic basalt-based glass–ceramics, Journal of the American Ceramic Society 82 (1999) 1181–1186.

[10] A.W.A. El-Shennawi, M.M. Morsi, G.A. Khater, S.A.M. Abdel-Hameed, Thermodynamic investigation on crystallization behaviour of pyroxenic basalt-based glasses, Journal of Thermal Analysis and Calorimetry 50 (1997) 53–560.